Geoderma 160 (2011) 457–467

Contents lists available at ScienceDirect

Geoderma

journal homepage: www.elsevier.com/locate/geoderma

A topographic template for estimating soil carbon pools in forested catchments

K.L. Webster [a], I.F. Creed [b,*], F.D. Beall [a], R.A. Bourbonnière [c]

[a] Natural Resources Canada, Canadian Forest Service, 1219 Queen St. E., Sault Ste. Marie, Ontario, Canada, P6A 2E5
[b] The University of Western Ontario, Department of Biology, 1151 Richmond Street, London, Ontario, Canada, N6A 5B7
[c] Environment Canada, Water Science & Technology Directorate, 867 Lakeshore Road, Box 5050, Burlington, Ontario, Canada, L7R 4A6

ARTICLE INFO

Article history:
Received 20 April 2010
Received in revised form 13 September 2010
Accepted 14 October 2010
Available online 13 November 2010

Keywords:
Topography
Soil
Carbon
Digital terrain analysis
Error
Uncertainty
Carbon accounting

ABSTRACT

There is a growing need to describe and quantify the heterogeneity in soil carbon pools in forests. In landscapes where topography is an important control on geomorphological, hydrological and/or biogeochemical processes, topographic features can be useful for partitioning the landscape into homogeneous units of soil carbon. Of particular interest are topographic features that are rare or cover a small proportion of the landscape but are disproportionately important in terms of soil carbon pools and/or fluxes. We developed an automated method for classifying topographic features by combining expert knowledge and a probabilistic approach. The topographic features were then used as a template from which to collect samples to estimate carbon of canopy leaves, freshly fallen litter, the forest floor, and the organic-rich A horizon or peat to a 5 cm depth within a small catchment of the Turkey Lakes Watershed of central Ontario. While the carbon in canopy foliage was homogeneous, there was significant heterogeneity in soil carbon pools among the topographic features, reflecting the importance of physical processes in shaping the distribution of soil carbon pools within this forested landscape. The catchment-aggregated estimates were under-estimated by 17% when only the dominant topographic feature was considered (i.e., 242 Mg C if backslope only used compared to 291 Mg C if all topographic features used). A Monte Carlo simulation method used to bound the uncertainty in soil carbon pools within each topographic feature resulted in catchment-aggregated estimates of 288 ± 56.0 (maximum probability) and 290 ± 51.3 Mg C (weighted probability) in the combined freshly fallen litter, forest floor, and the organic-rich A horizon or peat pool. The creation and application of this topographic template was useful for detecting, strategically sampling, and then mapping and scaling heterogeneity in soil carbon pools on the landscape.

1. Introduction

Predicting carbon pools is an important focus of national and international policies for inventory reporting and reviewing carbon emissions and removals (e.g., Land-use and Land-use Change and Forestry [LULUCF]). The Intergovernmental Panel on Climate Change (IPCC) reporting standards require that accounting systems provide carbon estimates and corresponding uncertainties that should be transparent, consistent, comparable, complete, accurate, verifiable and efficient (Watson et al., 2000). Developing methodologies that are consistent with IPCC standards is crucial for compiling data from finer jurisdictional levels (e.g., project, regional, provincial or state) for national compliance to international commitments. This paper contributes a methodology for improving estimates and corresponding uncertainties for soil carbon pools in forested landscapes.

In forested landscapes, topography is an important factor influencing soil carbon pools, particularly where other soil forming factors including climate, organisms, parent material and time are constant (Jenny, 1941). Topography influences soil properties through its effects on geomorphological, hydrological, and biogeochemical processes (Creed et al., 2002). Few soils develop in response to one-dimensional processes operating on flat, featureless land surfaces. Most soils develop in response to three-dimensional processes related to a hillslope, with soils from each topographic position connected by the continuous flow of water and the particulate and dissolved materials carried in the water. The hillslope represents the interplay between static factors (controlled by elevation, slope and aspect, which influence radiation, temperature and moisture at a specific site) and dynamic factors (relative position of the site within the hillslope, which influences the transport of particulate and dissolved materials downslope) (Young, 1972). Soils formed from a single material differ because of water transport processes that result in differential drainage conditions, differential transport and deposition of suspended materials, and/or differential leaching, translocation and redeposition of soluble materials (Hall and Olson, 1991). Theoretical frameworks that capture the interplay between static and dynamic factors on the hillslope have been developed that define distinct topographic features with similar soil forming properties along the hillslope catena (e.g., Conacher and Dalrymple, 1977).

* Corresponding author. Tel.: +1 519 661 4265; fax: +1 519 661 3935.
E-mail address: icreed@uwo.ca (I.F. Creed).

0016-7061/$ – see front matter © 2010 Elsevier B.V. All rights reserved.
doi:10.1016/j.geoderma.2010.10.016

Forest soil sampling schemes are often based on random or equal spacing, with little consideration of topography. Consequently, rare topographic features are not captured as frequently in soil surveys as topographic features that are more common. Although these rare topographic features comprise a small portion of the landscape, they may be hotspots with disproportionately higher rates of biogeochemical cycling than other areas on the landscape (McClain et al., 2003). To detect these small but potentially important features there is a need to design a spatially-explicit topographic template that identifies areas with similar biogeochemical responses (*sensu* Becker and Braun, 1999). Such a topographic template could provide a framework to (a) detect and locate rare topographic features; (b) strategically sample and monitor carbon pools, fluxes and environmental condition (e.g., temperature and moisture), and; (c) scale biogeochemical properties and function from a plot to the landscape.

The importance of topography in soil formation processes has led to the development of digital soil mapping methods that use topographic attributes derived from digital elevation models to predict soil properties (e.g., Bedard-Haughn and Pennock, 2002; Gessler et al., 2000; Moore et al., 1993; Ziadat, 2005). Many digital soil mapping methods use digital terrain attributes (e.g., slope, aspect, elevation, wetness index (Beven and Kirkby, 1979)) as predictors to describe soil properties in regression models. An alternative method that receives less attention is grouping terrain attributes into topographic features consistent with the theoretical framework of Conacher and Dalrymple (1977) using predefined geomorphological and hydrological criteria (MacMillan et al., 2000; Park and van de Giesen, 2004).

With these digital soil mapping methods, topographic features may have "crisp" boundaries in which there is a threshold between discrete values, or "fuzzy" boundaries in which there is overlap between continuous values. Fuzzy boundaries are based on expert knowledge of the key controls on soil forming processes and implemented through Boolean logic (Zhu and Band, 1994; Zhu et al., 2004). This latter approach provides a simple, yet sophisticated method of creating maps of topographic features with probabilistic boundaries that better represent the continuous spatial character and inherent complexity of soil properties (Qi et al., 2006). This approach also allows for the calculation of error or uncertainty in soil properties of interest.

The purpose of this research is to develop a digital soil mapping method for defining topographic features and to test how well it explains (or characterizes) heterogeneity in soil carbon, including total carbon pools within canopy green leaves, freshly fallen litter, the forest floor (litter, fibric, and hemic materials), and surface soils (0–5 cm in depth in mineral soil or peat). Specifically, we ask the following questions.

1. Can a topographic classification scheme adequately describe the topographic features of a small forest catchment?
2. Do soil carbon pools differ among topographic features?
3. How are catchment-aggregated estimates of soil carbon pools affected by the error in estimate of soil carbon pools and the difference in magnitude of soil carbon pools among topographic features?

The site for our study is a small (6.3 ha) catchment characterized by steep, predominantly northerly facing slopes terminating in a central wetland. The catchment (C38) is within the Turkey Lakes Watershed (TLW) in the Algoma Highlands of the Great Lakes–St. Lawrence forest region and has been a site of intensive hydrology and biogeochemistry research for the past 30+ years (Jeffries, 2002).

2. Methods

2.1. Study area

The Turkey Lakes Watershed (TLW) is a 10.5 km^2 experimental forest about 60 km north of Sault Ste. Marie, Ontario (Fig. 1). The climate is continental and is strongly influenced by the proximity of Lake Superior, with average annual precipitation and temperature of 1212 mm and 4.9 °C, respectively, for the period 1981 to 2005. Peak stream discharge occurs in April or May during snowmelt and again in October to November during autumn storms.

The watershed is located on the Precambrian Shield and is underlain by metamorphic silicate bedrock (greenstone) with small occurrences of granites (Jeffries and Foster, 2001). Shallow, bouldery, silt–loam ablation tills overlay compacted basal tills that cover the bedrock. Topography and relief (410 m) of the TLW is controlled by bedrock and contains rugged slopes terminating abruptly in depressions frequently containing deep peat deposits (>100 cm) that may be connected or disconnected from the drainage systems, forming topographic features with distinct physical, chemical, and/or biological properties. These include uplands (frequently dry), critical transition zones (intermittently wet due to the expansion of the wetland and upslope contributions during hydrologic events) and wetlands (frequently wet). Based on the Canadian soil taxonomy (Soil Classification Working Group, 1998), orthic Ferro-Humic and Humo-Ferric podzolic soils have developed with dispersed pockets of Ferric Humisols found in bedrock-controlled depressions and adjacent to streams and lakes.

The watershed is covered by an old growth (140 years and older (Jeffries et al., 1988)) hardwood forest, with a canopy dominated (>90%) by sugar maple (*Acer saccharum* Marsh.). Stand density (904 stems ha^{-1}), dominant height (20.5 m), diameter at breast height (15.3 cm), and mean basal area (25.1 m^2 ha^{-1}) are relatively uniform across the uplands, with stand density increasing and dominant height decreasing in the wetlands (Jeffries et al., 1988; Wickware and Cowell, 1985). Wetlands cover approximately 8% of the watershed, and most are treed swamps. The watershed has been free of recent human disturbance with the exception of a light selective harvest in the 1950s (Beall et al., 2001).

2.2. Defining topographic features

Conacher and Dalrymple's (1977) concept of a hillslope catena provided a theoretical framework for defining topographic features along hillslopes (Table 1). We implemented this theoretical framework to delineate topographic features using digital terrain analysis software (Terrain Analysis System 2.0.9; Lindsay, 2005). We developed a five-step method for quantifying the theoretical framework, adapting procedures previously developed (Lindsay and Creed, 2006; MacMillan et al., 2000).

Step 1: Hillslope topographic features which included crest, backslope, footslope and toeslope together with wetland (i.e., swamp in bedrock controlled depressions where significant peat accumulation occurred) were identified as potentially important features to characterize the landscape (Table 1).

Step 2: A 5 m digital elevation model (DEM) was generated from light detection and ranging (LiDAR) data (Lim et al., 2003a). LiDAR determines the elevation at the earth's surface by measuring the round-trip time of an airborne-fixed laser; this technique has a horizontal accuracy of 0.15 m in open canopy and 0.30 m under closed canopy (Lim et al., 2003b). LiDAR data were interpolated using an inverse distance weighted algorithm to 2.5 m and then re-sampled to 5 m using bi-linear re-sampling method (Lindsay, 2005). Of the nine terrain derivatives derived from DEMs that were proposed by MacMillan et al. (2000) to represent topographic characteristics, five terrain derivatives were selected and derived from the 5 m DEM for this classification (Table 2): (a) percent height relative to local pits and peaks; (b) percent height relative to local channels and divides; (c) wetness index; (d) slope curvature; and (e) slope gradient. For (a) and (b), the relative position was calculated using an eight direction flow algorithm (D8, which directs flow to the steepest downslope cell (O'Callaghan and Mark, 1984)), on a DEM where single pits were removed (for pit to peak) or entire depressions were removed (for channel and divide) (Planchon and Darboux, 2002). Channels were defined using the D8 flow algorithm, and channel initiation was set at

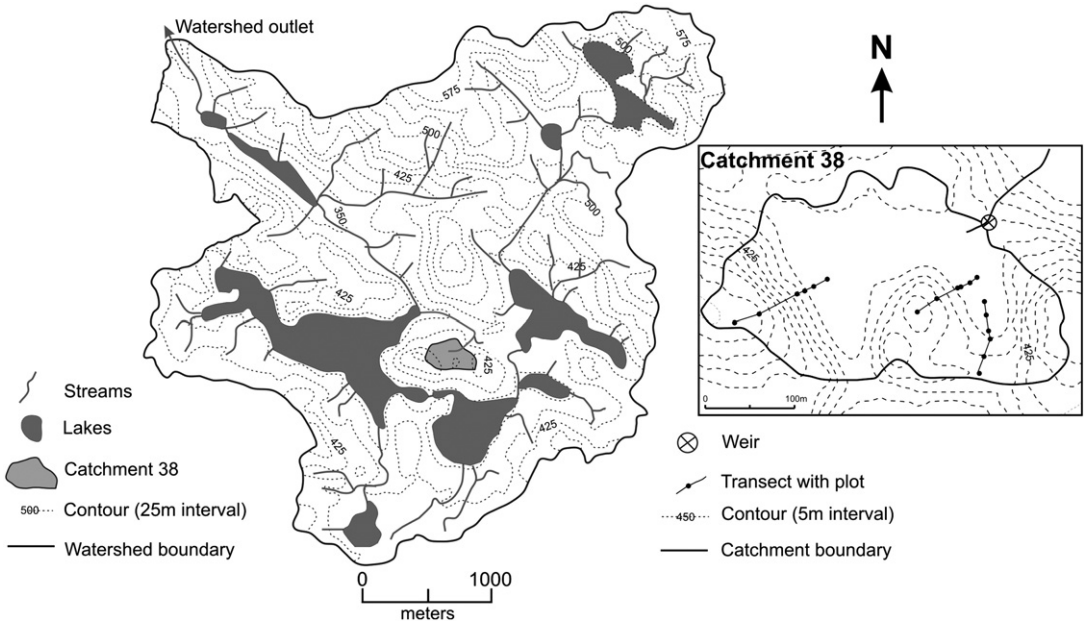

Fig. 1. The Turkey Lakes Watershed centered at 47° 03' N and 84° 25' W, with the location of catchment C38 highlighted.

a threshold of 8100 m^2 from the specific contributing area layer on a depression filled DEM based on knowledge of the location of the drainage network within the watershed. For (c), the wetness index was calculated as the natural logarithm of specific contributing area using the infinite direction (Dinf) flow algorithm (which partitions flow to downslope cells proportional to the flow angle (Tarboton, 1997)) divided by the local slope. For (d), slope curvature was calculated as the rate of change of slope in the downslope direction on a 3×3 moving window, with negative values for slopes increasing downhill (convex flow profile) and positive values for slopes decreasing downhill (concave profile) (Wilson and Gallant, 2000). For (e), slope gradient was calculated as the rate of change of slope in the downslope direction on a 3×3 moving window (Wilson and Gallant, 2000).

Step 3: The five terrain derivatives were converted from "crisp" to "fuzzy" through the application of a fuzzy membership function, where the shape of the probability function is determined by the attribute values where it has complete membership (i.e., the central concept, b) and the rate of decline in membership (i.e., its dispersion, d) as defined by experts (Fig. 2). "Upper" and "lower" models were used for computing attributes at the upper and lower extremes of the distribution of values for a particular terrain derivative. A "central" model was used for computing attributes that were near the middle of the distribution of values for a particular terrain derivative. For example, the terrain derivative of profile curvature was converted to the fuzzy attribute of convex using the lower bounded membership function, whereas concave used the upper bounded and planar the central bounded distributions (Table 3).

Table 1
Description of soil forming functions of topographic features (modified from Conacher and Dalrymple, 1977).

Topographic feature	Topographic description	Soil forming functions
Crest	Flat area at the top of ridge	Vertical leaching Infiltration, groundwater recharge
Backslope	Steep area at the middle of the hillslope	Transport of material by flow, slump, slide, raindrop impact and surface wash Lateral flows
Footslope	Moderately sloped transitional area between steep upland and gentle sloped lowland	Colluvial deposition from upslope Infiltration, throughflow, saturation excess overland flow, return flow
Toeslope	Flat to gently sloped area at the base of the hillslope	Depositional area from alluvial materials, subsurface water flows in both directions Alluvial deposition from upslope Infiltration, throughflow, saturation excess overland flow, return flow
Wetland	Flat, saturated area	Frequently inundated Groundwater discharge Ponding, saturation excess overland flow, channel flow

Table 2
Terrain derivatives, their description and the processes that define them (modified from MacMillan et al., 2000). Terrain derivatives used in the current study are highlighted in gray.

Topographic derivative	Topographic description	Soil forming functions
Elevation relative to maximum elevation of study area	Position in watershed	Relative landscape position in watershed
Elevation relative to peak & pit	**Position on slope**	**Relative landscape position along hillslope**
Elevation relative to channel & divide	**Position on slope**	**Relative landscape position along hillslope**
Absolute height above pit	Position on slope	Absolute landscape position along hillslope
Absolute pit to peak height	Position on slope	Absolute landscape position along hillslope
Wetness index	**Local slope and position on slope**	**Relative drainage conditions (spatial distribution and extent of zones of saturation)**
Profile curvature	**Local slope shape**	**Flow acceleration, erosion/deposition rate**
Plan curvature	Local slope shape	Flow acceleration, erosion/deposition rate
Slope gradient	**Local slope**	**Overland and subsurface flow velocity and runoff rate**

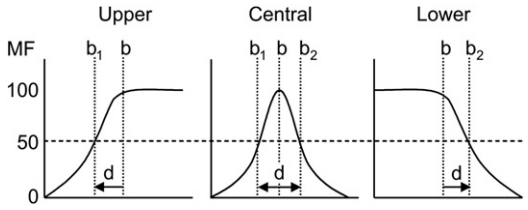

Fig. 2. Fuzzy semantic import models used in converting terrain derivatives into fuzzy terrain attributes based on membership function (MF), where the shape is determined by maximum probability (b) and its dispersion (d) (adapted from Burrough et al., 1992).

Step 4: Fuzzy attributes were combined to define the topographic features based on extensive field experience of scientists working in the watershed. A function was created from the set of fuzzy attributes (Table 4), with each fuzzy attribute having a weight, and combined weights summing to one (MacMillan et al., 2000). Multiple definitions of a feature were possible. For example crest was defined by the fuzzy attributes of near divide and near level *or* near peak and near level. A map was created for each topographic feature with each grid cell assigned the probability of belonging to that feature. The individual maps were reclassified by assigning a given grid cell to the topographic feature with the highest probability of all the topographic feature maps.

Step 5: Wetlands were not identified using fuzzy attributes. Instead, a probabilistic approach that determines the likelihood of an area being flat or in a depression was used to delineate the wetlands (Lindsay and Creed, 2006). This approach recognizes that DEMs contain elevation errors and that a flat or depression is likely to exist if the elevation difference between neighboring grid cells is greater than the elevation error term. A random error term is added to the DEM, depressions in the DEM are filled (Planchon and Darboux, 2002), and each grid cell modified by the depression filling process is flagged. This process is repeated by using random error terms selected from a distribution with a mean of zero and a standard deviation equal to the vertical accuracy of the DEM (i.e., 0.3 m). A probability of occurrence of being flat or in a depression is calculated by the number of times each grid cell is identified as a flat or depression (p_{dep}). A probability map is produced (0 = zero probability of being a wetland; 1 = 100% probability of being a wetland). A critical threshold in the probabilities of ≥0.2 was applied to delineate the wetland (Lindsay and Creed, 2006), and a 3×3 gamma filter was applied to remove embedded single grid cells that were mapped as non-wetlands (Clark et al., 2009). This probabilistic approach is useful in detecting wetlands (Creed et al., 2008) and superior to other approaches (e.g., a threshold in slope, below which a grid cell is defined as a wetland (Creed et al., 2003)).

2.3. Soil carbon pools

Soil carbon pools were sampled along three hillslope transects with each hillslope containing the four upland topographic features (crest, backslope, footslope, toeslope) and the wetland topographic feature (center, where paludification has elevated the peat, and periphery, where the peat surface is lower) ensuring adequate coverage of the catchment and replication of the topographic features (Fig. 1).

Soil carbon substrates were sampled that reflected a range in ages of organic matter (Bourbonnière and Creed, 2006), including (a) green leaves representing the youngest carbon pool which enters the soil following precipitation events; (b) freshly fallen leaves representing a relatively young (<1 year) carbon pool that is available for decomposition at the start of the next growing season; (c) forest floor including the litter layer (1 year old material composed of the partially decomposed leaves from the previous year), the fibric layer (2–3 years old material composed of fragmented leaves collected below the litter), and the hemic layer (4+ years old material composed of degraded leaves collected below the fibric layer), as well as fine roots that grew within the forest floor; and (d) the organic-rich A horizon or peat, to a maximum depth of 5 cm (Bourbonnière and Creed, 2006).

For green leaves, carbon pools were estimated by multiplying the mean leaf area index (LAI) by the specific leaf area for sugar maple (36.3 $m^2\ kg^{-1}$ C) (White et al., 2000). LAI was determined by taking nine consecutive radiation measurements within each topographic feature with a Li-Cor LAI-2000 meter (Li-Cor, 2004) and corrected with open site radiation measurements from a nearby clearing. This optical sensor measures canopy gap fraction by detecting blue (400 to 490 nm) diffuse light penetrating the canopy at five concentric rings, corresponding to 0–13° (ring 1), 16–28° (ring 2), 32–43° (ring 3), 47–58° (ring 4), and 61–74° (ring 5) zenith angles (Li-Cor, 2004). The LAI was calculated from the LAI-2000 measurements using Eqs. (2.1) to (2.3).

$$LAI = 2\sum_{1}^{5} \overline{K}_i W_i \tag{2.1}$$

Where $\overline{K}_i$ is the mean contact number for the *i*th ring and W_i is the weighting factor for the *i*th ring.

$$\overline{K}_i = \frac{\frac{1}{n}\sum_{j=i}^{n} -ln\left(\frac{B_j}{A_j}\right)}{S_i} \tag{2.2}$$

Table 3
A description of the fuzzy attributes used in the topographic feature classification and the fuzzy semantic import model and parameter used to define them. The b1 and b2 are the upper and lower limits, respectively, of the dispersion (d) from the maximum probability.

Fuzzy attribute	Description	Units	Topographic derivative derived from	Model	b1 and/or b2	d
Near divide	Near local divide	%	Elevation relative to channel & divide	Upper	75	15
Near peak	Near local peak	%	Elevation relative to channel & divide	Upper	75	15
Near mid	Near peak to pit midslope	%	Elevation relative to peak & pit	Central	25, 75	25
Near channel	Near local channel	%	Elevation relative to channel & divide	Lower	10	5
Near pit	Near local pit	%	Elevation relative to peak & pit	Lower	10	5
High WI	High wetness index	m^2/°	Wetness index	Upper	6.5	3
Convex D	Convex in profile curvature (+'ve curvature)	°/100 m	Profile curvature	Lower	-2	1
Concave D	Concave in profile curvature (-'ve curvature)	°/100 m	Profile curvature	Upper	2	1
Planar D	Planar in profile curvature (~0 curvature)	°/100 m	Profile curvature	Central	-2, 2	2
Near level	Nearly level slope (1.5° to 5°)	%	Slope gradient	Lower	8.8	6.2
Relatively steep	Not level (>5°)	%	Slope gradient	Upper	8.8	8.8

Table 4
The fuzzy attributes and weights used to define each of the topographic features. Multiple rows occur for each feature indicating their alternative definitions.

Topographic feature	Near divide	Near peak	Near mid	Near channel	Near pit	High WI	Convex D	Concave D	Planar D	Near level	Relatively steep
Crest	50									50	
		50								50	
Backslope	50						50				
		50					50				
			50						50		
Footslope						25		25			50
				50				50			
					50			50			
Toeslope				50					50		
					50				50		
Wetland	Defined by stochastic depression analysis using root mean square difference = 0.001, root mean square error = 0.3 and probability of depression (p_{dep}) ≥ 0.2.										

Where n is the total number of observations j, B is the below-canopy observation and A is the above-canopy observation, and S is the path length.

$$W_i = \Delta\theta_i \; sin \; \overline{\theta}_i \tag{2.3}$$

Where $\overline{\theta}_i$ is the mean zenith angle, and $\Delta\theta_i$ is the ring width (radians) associated with the ith ring. To minimize the effects of multiple scattering of light within the canopy on the LAI-2000 measurement, rings 4 and 5 were removed in the post-processing (Chen et al., 2006).

For freshly fallen leaves, six samples at each topographic feature and for the center and periphery of the wetland topographic feature were collected on a 30 cm × 30 cm mesh placed on the surface of the forest floor prior to leaf fall and collected prior to snowpack development. Freshly fallen leaves samples were dried at 25 °C, analyzed for carbon concentrations (%) with a Carlo-Erba NA2000 analyzer (Milan, Italy), and converted to carbon pools (g C m^{-2}) by multiplying carbon concentration (g C g^{-1}) by litter mass (g m^{-2}).

For forest floor, six samples were collected at each topographic feature and for both the center and periphery of the wetland topographic feature by cutting 15 cm × 15 cm blocks of the entire layer. Forest floor samples were dried at 25 °C and analyzed for carbon concentrations (%) with a Carlo-Erba NA2000 analyzer (Milan, Italy). Forest floor samples collected at the same time were dried at 60 °C, weighed and measured. Forest floor carbon pools were calculated by multiplying carbon concentration (g C g^{-1}) by bulk density (g m^{-3}) and then by depth (m).

For soils, six samples of the A horizon soil up to 5 cm depth (i.e., maximum depth of A horizon) were collected at each of the upland topographic features with an open-sided sampler (40 cm × 4.4 cm I.D.) (for carbon analysis) or a split core sampler (32 cm × 4.8 cm I.D.) (for bulk density determination; stones >2 mm were removed and weighed to correct bulk density for coarse fragment content). Six peat samples from the top 5 cm were also collected at both the center and periphery of the wetland topographic feature with a Jeglum sampler (7.6 cm × 7.6 cm × 50 cm) (Jeglum et al., 1992). Soil samples were dried at 25 °C (for chemical analyis), 60 °C (for bulk density of organic soil), or 105 °C (for bulk density of mineral soil). Soil samples were analyzed for carbon concentrations (%) with a Carlo-Erba NA2000 analyzer (Milan, Italy) and converted to carbon pools (g C m^{-2}) by multiplying carbon concentration (g C g^{-1}) by bulk density (g m^{-3}) and then by depth (m).

Sampling for the study occurred in 2004 (forest floor and soil) and 2005 (green leaves, freshly fallen leaves, forest floor, and soil). Samples were collected from each of the replicated topographic features for each of the carbon pools (for green leaves n = 1; for freshly fallen leaves n = 5; for forest floor n = 6, three in each year; for soil n = 6, three in each year). Green leaf samples represented maximum canopy leaf biomass during the summer season. Freshly fallen leaf samples represented maximum canopy leaf fall during the autumn season. Forest floor and soil samples were collected over 2 years, with no significant differences in carbon pools observed between the 2 years (p = 0.12 for forest floor and p = 0.58 for A horizon/peat). In the absence of soil samples collected on an annual basis, it was assumed that the green leaves, freshly fallen leaves, forest floor, and soil carbon pools were relatively stable, with spatial heterogeneity more important than temporal variability.

2.4. Relating topographic features to soil carbon pools

Soil carbon pools among topographic features were compared using one-way analyses of variance (ANOVAs) or ANOVAs on ranks (non-parametric data). Statistical significance ($p < 0.05$) was assessed by pair-wise comparison tests (Tukey's for parametric and Dunn's for non-parametric data). Statistical tests were performed in SigmaPlot (ver. 11, Systat Software Inc, 2008).

Aggregation of soil carbon pools within the catchment was calculated by (a) a simple method of applying the topographic feature with the highest probability to each grid cell, and (b) a more complex method of applying the topographic features as a weighted average of their probabilities. The two methods were compared to determine how uncertainty in the classification of a topographic feature affected the aggregated estimate. Continuous maps of the distribution of soil carbon pools were created by reclassifying each of the 25 m^2 grid cells within the catchment based on the values from the weighted average.

Uncertainty in the estimates of the aggregated soil carbon pool introduced by heterogeneity in soil carbon pools within topographic features was assessed using a Monte Carlo simulation method for each of the maximum probability and weighted average approach). For each of 100 iterations, values for the pools for each grid cell were sampled from a normal distribution between their upper and lower standard deviations using the norminv (rand(), mean, standard deviation) function within Microsoft Office Excel (Microsoft Corporation, 2003). The soil carbon pools were summed for all grid cells in the catchment for each of the iterations and the mean and standard deviation calculated from the 100 catchment-aggregated iterations.

3. Results

3.1. Topographic features

The catchment was composed of a variety of topographic features that were hidden under a relatively homogeneous canopy of sugar maple (Fig. 3A, Table 5). Based on assignment of maximum probability (Fig. 3B), the catchment was dominated by uplands (60.2%, including 5.5% crest and 54.7% backslope) and wetlands (25.1%). The transition zone between the upland and wetland occupied the least area (14.8%), with a 1:2 ratio of footslope (4.9%) and toeslope (9.9%). Inspection of the

location and extent of these features in the field confirmed that the classification was successful in delineating the topographic features.

The probability of a topographic feature provides an indicator of confidence that any particular location is that topographic feature (Fig. 3C–G). Probabilities of the assigned topographic features ranged from 49 to 100%, with 50% of the grid cells having a maximum probability greater than 75% (Fig. 3B). Areas that clearly met the criteria of the topographic features were predicted with greater accuracy, whereas areas at the boundary between different topographic features (e.g., between crest and backslope and between backslope and footslope) were predicted with lower accuracy.

Table 5
The area of topographic features within catchment C38.

Topographic feature	Area (m^2)	Area (%)
Crest	3450	5.5
Backslope	34,650	54.7
Footslope	3100	4.9
Toeslope	6250	9.9
Wetland	15,850	25.1
Total	63,300	100

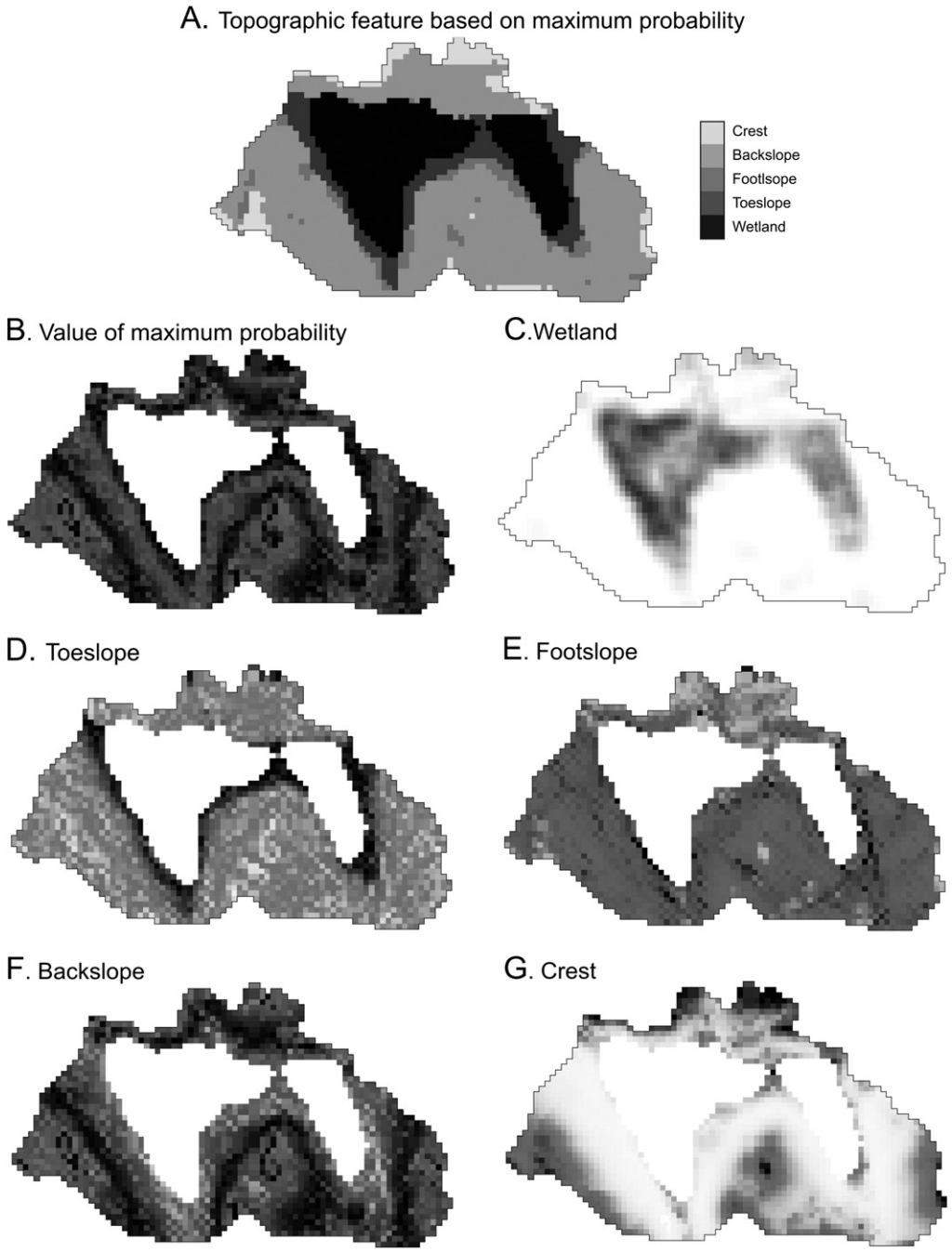

Fig. 3. Topographic features for catchment C38 based on highest probability (A) and the value of maximum probability (B). Panels C through G indicate distribution of probabilities for wetland (C), toeslope (D), footslope (E), backslope (F), and crest (G). Grey-scale shading in panels B–G indicates probability from 0 (white) to 1 (black). Wetland is masked out in panels B, D–G.

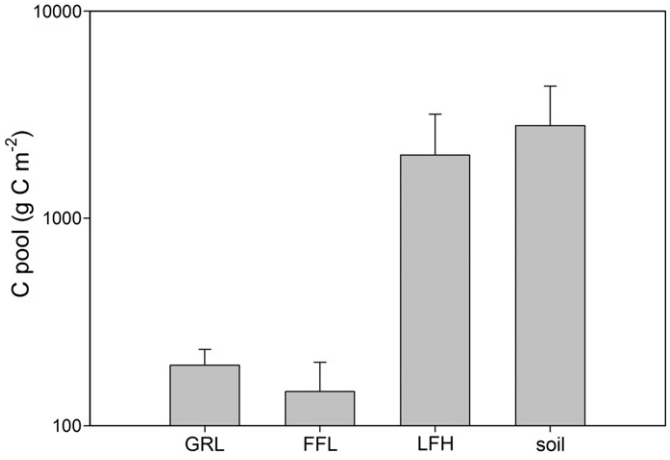

Fig. 4. Mean carbon pools (±standard deviation) contained within green leaves (GRL, n = 18), freshly fallen leaves (FFL, n = 90), forest floor (LFH, n = 108), and top 5 cm layer of mineral soil or peat (soil, n = 108). Note that the y axis is on a log scale.

3.2. Soil carbon pools

The size of the measured soil carbon pools across all topographic features increased from the green leaves and freshly fallen leaves (196 and 146 g m^{-2}, respectively) to the forest floor (2020 g m^{-2}) and mineral soil (soil, 2800 g m^{-2}) (Fig. 4).

There was no significant difference in the green leaves carbon pool among the topographic features ($p = 0.173$), but there was in the freshly fallen leaves, forest floor, and soil carbon pools (Table 6).

The freshly fallen leaves carbon pool changed along the hillslope ($p < 0.001$), with a large pool in footslope features (197 g m^{-2}), moderate pools in the toeslope and crest features (163 and 147 g m^{-2}), and the smallest pool in the backslope and wetland features (123 and 124 g m^{-2}). The greatest variability in freshly fallen leaves occurred within the toeslope, footslope and backslope features, with sample standard deviations of 53.1, 60.3 and 59.1 g C m^{-2} respectively.

The forest floor carbon pool also changed along the hillslope, although the pattern was not consistent with that of freshly fallen leaves. A larger pool was recorded in the wetland (2980 g m^{-2}) than the upland features (range of 1260 to 1360 g m^{-2}). In the upland, the forest floor carbon pools were small despite the pattern in freshly fallen leaves, while in the wetland, despite small freshly fallen leaves carbon pools, the forest floor carbon pools were large and variable (25th to 75th percentile range of 2160 to 3980 g C m^{-2}).

The soil carbon pool differed from both the freshly fallen leaves and forest floor. The soil carbon pool was heterogeneous both within and among topographic features. Within the soil, the largest pool occurred at the crest (3350 g C m^{-2}) and the smallest pool in the wetland and footslope (2140 and 2070 g C m^{-2}), and intermediate topographic features were not significantly different from either of the extreme positions (range of 2440 to 2790 g C m^{-2}). The soil carbon pool was particularly heterogeneous in the toeslope feature (25th to 75th percentile range of 2060 to 5150 g C m^{-2}).

3.3. Relating topographic features to soil carbon pool

Contiguous maps of soil carbon pools were created using the probabilities of topographic features as weighted averages (Fig. 5A–D). Aggregating the soil carbon pools by topographic feature (Table 7) showed that the backslope was the single largest contributor to soil carbon pools in the catchment due to its large extent, despite having lower density of soil carbon.

The relatively simple *vs.* complex method for calculating aggregated soil carbon pool estimates produced similar results (Table 8). The estimates calculated using the topographic feature with highest probability were slightly lower than the estimates based on the weighted average of probabilities for each of the soil carbon pools, but these differences were small and well within the bounds of error determined from the Monte Carlo simulations (Table 7).

Errors in the catchment-aggregated estimates differed among soil layers (Table 8). Errors were smaller for freshly fallen leaves and forest floor (22 and 20% respectively) and larger for the soil carbon pool in the top 0–5 cm of mineral soil or peat (26%), due to large within-feature heterogeneity (Table 8, Fig. 6). When all pools were combined, the mean total soil carbon pool for the catchment was estimated at 288 ± 56.0 Mg C for the Monte Carlo simulation using maximum probability of topographic features and 290 ± 51.3 Mg C for

Table 6
Summary of ANOVA results for evaluating statistical differences in carbon pools at crest, backslope, footslope, toeslope and wetland (combining center and periphery) for each of three hillslopes. Carbon (g m^{-2}) in green leaves and freshly fallen leaves based on ANOVA, and carbon (g m^{-2}) in forest floor and A horizon or peat to maximum depth of 5 cm based on ANOVA on ranks due to non-parametric nature of the data. Topographic features with different letters are significant at $p < 0.05$ using Tukey's test for parametric data and Dunn's method for non-parametric data.

Carbon (g m^{-2})	n[1]	Statistic	Crest	Backslope	Footslope	Toeslope	Wetland
Green leaves	18	Median	185	208	217	208	190
$p = 0.173$		25%	151	201	193	193	143
		75%	208	244	235	253	199
		Sig. diff.	a	a	a	a	a
Freshly fallen leaves	90	Mean	147	123	197	163	124
$p < 0.001$		Std. deviation	43.1	59.1	60.3	53.1	42.8
		Std. error of estimate	11.1	15.3	15.6	13.7	7.8
		Sig. diff.	ab	a	b	ab	a
Forest floor	108	Median	1260	1340	1360	1360	2980
$p < 0.001$		25%	980	1010	1120	1100	2160
		75%	1920	1880	1790	1670	3980
		Sig. diff.	a	a	a	a	b
Soil $p = 0.003$	108	Median	3350	2440	2070	2790	2140
		25%	2250	1270	1430	2060	1920
		75%	4610	3440	2930	5150	2270
		Sig. diff.	b	ab	ab	b	a

[1] Sample size (n) represents total number of samples for all hillslopes. For green leaves, n = 18 reflects one sample for each of four upland topographic features and two wetland (periphery and center) topographic features for each of three hillslopes. For freshly fallen leaves, n = 90 reflects five samples for each of six upland and wetland topographic features for each of three hillslopes. For forest floor and soil, n = 108 reflects six samples for each of six upland and wetland topographic features for each of three hillslopes.

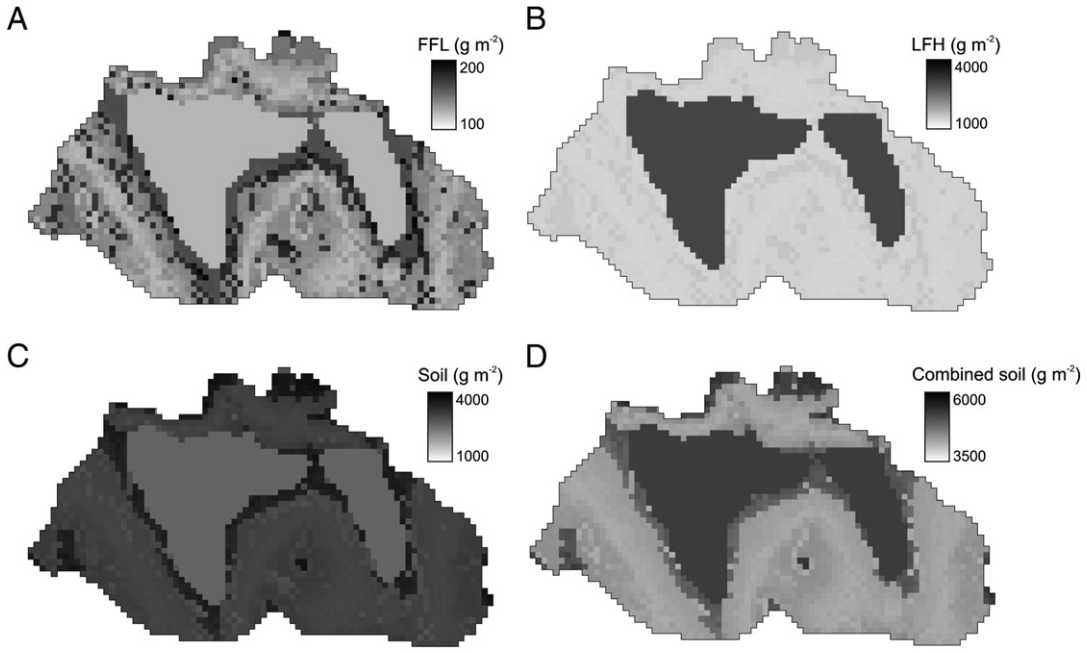

Fig. 5. Maps of soil carbon pools of freshly fallen leaves (FFL) (A), forest floor (LFH) (B), soil (C), and combined soil (D) for catchment C38.

the Monte Carlo simulated using weighted probability of topographic features (Table 8).

4. Discussion

Soil carbon pools are inherently heterogeneous, but developing accurate estimates of soil carbon pools is important for understanding the strength of forests as carbon sinks. Herein, we present a soil-landscape modeling approach that *a priori* combines topographic attributes into topographic features in a probabilistic manner to partition the landscape into similar carbon response units. Using this spatially-explicit topographic template allows us to strategically sample and map soil carbon pools and fluxes and estimate error. Soil-landscape modeling techniques, similar to the one used here, have been useful for creating distinct spatial units to characterize different geomorphological, hydrological and biogeochemical processes of other landscapes (e.g., Park and van de Giesen, 2004; Park et al., 2001; Pennock et al., 1987; Schmidt and Hewitt, 2004). However, this study is the first to use this approach to strategically sample soil carbon from different horizons, scale carbon pools to a larger catchment area and estimate error.

4.1. Heterogeneity in soil carbon pools both within and among topographic features

The magnitudes of the soil carbon pools calculated in this study were comparable to previous studies within the TLW. Random sampling in the TLW by Morrison and Foster (1992 [quoted in Johnson and Lindberg, 1992]; 2001) found pools of freshly fallen leaves, the forest floor, and the top 7 cm of mineral horizon (composed of A and B horizons) to be 216, 1650 and 2238 g C m^{-2}, respectively. Although the topographic position from which these samples were taken was not known, they were in the range of the upland topographic features of catchment C38.

Our study found that under the homogenous canopy, heterogeneity in soil carbon pools was significant. Not only did the distribution of soil carbon pools vary along the hillslope, the pattern differed between horizons. This suggested that different geomorphological, hydrological and/or biogeochemical processes operated on each of the carbon pools.

For freshly fallen leaves, the pattern of higher accumulation in the depositional areas within the critical transition zone and lower accumulation in erosional areas of the backslope may be due to redistribution of the freshly fallen leaves, with their low mass and large surface area, by wind (Orndorff and Lang, 1981). Also, given that the crests have a relatively large freshly fallen leaves pool while also being most exposed to wind, the relative paucity of freshly fallen leaves on backslopes may be due to wind and water movement (Xiong and Nilsson, 1997). Because of the small mass of freshly fallen leaves, it is often disregarded in soil analyses; in fact, to our knowledge this is the first study to examine the topographic controls on this pool of soil carbon. While insignificant in the portion of soil mass it represents, this pool is important substrate for microbial respiration (Webster et al., 2008a,b), and thus understanding its distribution will be important for understanding the atmospheric fate of carbon. In this study, analysis of freshly fallen leaves distribution was simplified by the homogeneity of sugar maple canopy. However, in multi-species catchments, the distribution of freshly fallen leaves may be confounded due to differences in foliar chemistry (affecting

Table 7
Topographic feature-integrated pools of soil carbon (Mg C) for freshly fallen leaves, forest floor, soils, and their combination for catchment C38 in the Turkey Lakes Watershed using topographic feature with highest probability.

Topographic feature	Freshly fallen leaves (Mg C)	Forest floor (Mg C)	Soil (Mg C)	Combined (Mg C)
Crest	0.51	5.39	12.2	18.1
Backslope	3.95	44.8	83.9	133
Footslope	1.04	10.2	18.6	29.8
Toeslope	0.90	7.91	18.8	27.6
Wetland	1.96	48.5	32.7	83.1

Table 8
Catchment-aggregated pools of soil carbon (Mg C) for freshly fallen leaves, forest floor, soils, and their combination using topographic feature with the highest probability (maximum probability), weighted by probabilities of all features (weighted probability), and estimated from Monte Carlo simulation that takes into account the heterogeneity in the carbon pool within a topographic feature (Monte Carlo simulation).

Pool	Catchment-aggregated pool			
	Maximum probability	Weighted probability	Monte Carlo Simulation with maximum probability (±standard deviation)	Monte Carlo Simulation with weighted probability (±standard deviation)
Freshly fallen leaves (Mg C)	8.36	8.88	8.86 ± 2.28	9.07 ± 2.03
Forest floor (Mg C)	117	118	119 ± 25.5	119 ± 24.3
Soil (Mg C)	166	167	161 ± 47.5	162 ± 43.3
Combined (Mg C)	291	294	288 ± 56.0	290 ± 51.3

decomposition rates), mass (affecting mobility) and leaf retention (affecting input of litter) (Finzi et al., 1998; Li et al., 2010). Furthermore, the redistribution of freshly fallen leaves may also have a high degree of inter-annual variation, due to differences in weather patterns. For example, changes in photosynthetically-active radiation, temperature and precipitation may affect leaf production (Churkina and Running, 1998) and wind and precipitation may affect post-senescence movement of leaves on the hillslope (Lee et al., 1999).

The pattern in freshly fallen leaves was disconnected from the forest floor. In the upland, forest floor carbon pools were small, suggesting this young pool is also labile and quickly decomposed. In contrast, in the wetland, forest floor carbon pools were large. Saturated and reducing conditions that occur for most of the year in the wetland would limit decomposition and allow litter to accumulate (Laiho, 2006). Furthermore, the forest floor forms a spongy and interconnected mat of partially decomposed material. This highly porous structure would result in vertical infiltration and leaching (Lauren and Mannerkoski, 2001), which could be an important mechanism for transport and transformation within this pool.

The soil carbon pool in the surface (0–5 cm) organic-rich mineral and peat horizons is likely influenced by infiltration, but also by shallow, subsurface lateral flows from the upslope contributing areas (Rosenbloom et al., 2006). Crest areas accumulate soil carbon in the surface mineral horizon because they are flat and there is minimal lateral transport that would move soil carbon downslope from these flat areas. Backslope and footslope accumulate less soil carbon because they are steeper and have

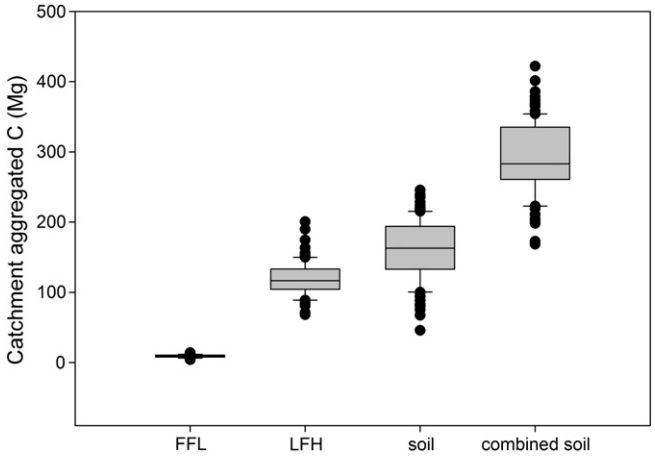

Fig. 6. Box plots of Monte Carlo simulated estimates of carbon pools over 100 iterations based on weighted probability of the soil being assigned to a specific topographic feature. The box represents the bounds of 25th, 50th (median), and 75th percentiles, and the bars indicate the 10th and 90th percentiles. Dots indicate extreme values outside the 10th and 90th percentiles.

greater lateral flows. Toeslope areas accumulate various amounts of soil carbon; this topographic feature situated at the base of the hillslope is where differences in flow length and contributing area would be most pronounced, perhaps explaining the heterogeneity of soil carbon within this feature. Wetland areas accumulate moderate soil carbon pools. The loss of momentum in the flat area of the wetland prevents large inputs of upslope matter to the wetland and the lower density of organic material within the surface peat horizons in the wetland both contribute to the smaller magnitude in this soil carbon pool. Our findings are supported by others who have found relationships between flow accumulation *vs.* dispersion areas and soil carbon pools (e.g., Gessler et al., 2000; Martin and Timmer, 2006; McKenzie and Ryan, 1999).

The soil carbon pools contained within the surface organic-rich mineral and peat horizons have shorter residence times (Gaudinski et al., 2000). Some of the heterogeneity in these more dynamic pools is also likely linked to biological factors including heterogeneity in soil respiration. Webster et al. (2008a) found the toeslope and footslope areas to be major sites of soil respiration because of the synchronicity in optimal temperature and moisture conditions during the growing season and the high quality of substrate found there. Other biological factors such as community composition and productivity may have weaker relationships to topography. Changes in soil carbon pools related to differences in vegetation composition are well established (e.g., Benayas et al., 2004; McKenzie and Ryan, 1999; Rezaei and Gilkes, 2005), but even with homogeneity in the overstorey canopy, there may be sufficient heterogeneity in the understorey to affect litter inputs into the organic and upper mineral soil (Benayas et al., 2004). Zushi (2006) found a positive relationship of soil carbon pools to openness, and McKenzie and Ryan (1999) found that a normalized difference vegetation index helped explain variation in soil carbon. The heterogeneity may also be confounded by the legacy of biology (e.g., inputs of coarse woody debris from past disturbance [Martin and Timmer, 2006]) that may leave a mark but not be presently observed.

Studies that integrate soil carbon with depth ignore the contribution of individual soil horizons. Quantifying soil carbon pools in the horizons separately allows for consideration of different carbon residence times in the integrated soil carbon pool. For example, if a higher proportion of the soil carbon pool is stored in short-residence time pools (e.g., freshly fallen leaves or forest floor), this may lead to a more rapid feedback to the atmosphere with climate change than if the soil carbon was contained within pools stabilized within the mineral horizon (Webster et al., 2008a,b).

4.2. Topographic based scaling of soil carbon pools

At the catchment–scale, the backslope was the single largest contributor to soil carbon pools due to its large extent, despite having low density of soil carbon. However, on a per topographic feature basis, the footslope, toeslope and wetland features had soil carbon pools that

were disproportionately larger. If these features were not sampled (as was likely the case in earlier estimates of soil carbon pools within the TLW [e.g., Morrison, 1990; Morrison and Foster, 2001]), then catchment-aggregated estimates would have been considerably lower. For example, if we take the dominant topographic feature as representative (i.e., backslope), then the catchment aggregated soil carbon pool would be 242 Mg C. This is 17% lower than the estimate of 291 Mg C calculated when all topographic features (i.e., crest, backslope, footslope, toeslope and wetland) are included using the maximum probability approach. The implication is that we under-represent the soil carbon pools by not using a topographic feature based approach. In fact, failure to include different topographic features is more influential than the estimate of errors in classifying the topographic features (i.e., 291 Mg C if maximum probability of topographic feature used *vs.* 294 Mg C if weighted probability of topographic features used, Table 8). This emphasizes the importance of a topographic-feature based approach to estimating soil carbon pools within catchments.

The topographic template approach enables both the uncertainty in the classification of topographic features and the inherent heterogeneity of soil properties within and among topographic features to be taken into account. The probabilities of the assigned topographic features (e.g., Fig. 3B) indicate how well the catchment topography has been classified and where additional topographic features may be required. From these probabilities, continuous maps of soil carbon pools can be created based on the similarity of a location to a specific topographic feature thus showing gradual changes in soil carbon pools at the boundaries between topographic features. However, if a weighted or maximum probability is used, discrete maps of soil carbon pools are created. The weighted probability approach provided intuitive maps of the distribution of soil carbon pools within the catchment; however, the simpler approach using the maximum probability (that did not account for uncertainty in topographic features) produced similar catchment-aggregated estimates of soil carbon pools. Furthermore, combining the topographic features with a Monte Carlo simulation method that accounts for variability in soil carbon within a topographic feature provided a means to bound the error in catchment-aggregated estimates.

The topographic template performed well in capturing the variation in soil carbon pools within a small, first-order catchment. While there was no independent validation of the results in space (i.e., in other catchments) or in time (i.e., multiple years), it is expected that the key terrain derivatives are likely applicable to most catchments, although the fuzzy boundaries and weights (e.g., Tables 3 and 4) may need to be adjusted based on local topography. Moving from the catchment to watershed scale, differences in contributing area that affect the amount of water and its rate of transfer and differences in aspect that affect the amount of intercepted solar radiation and thereby soil moisture and temperature may become important (Gessler et al., 2000). Furthermore, at the regional scale, differences in slope, aspect, and elevation that affect radiation, temperature and precipitation may become important (Park and Vlek, 2002). Future studies will investigate how these additional topographic controls influence soil carbon pools across this hierarchy of scales.

5. Conclusion

All topographic features, including those that are rare but biogeochemically important, should be sampled when estimating catchment–scale soil carbon pools. To do this we proposed a topographic based approach that provides a template not only for strategic sampling and monitoring, but also for mapping and scaling both the magnitude and uncertainty in estimating the magnitude of carbon pools. Failure to include this heterogeneity may lead to over- or under-estimation of soil carbon pools. Methods that account for heterogeneity and assess the uncertainty in carbon pool magnitude will become increasingly necessary as national and international policies for reporting changes in carbon pools that accompany changes in land cover and land-use are implemented. Understanding controls on soil carbon pools at catchment scales is the first step to understanding carbon dynamics at broader scales, and future work must further consider the changing nature of topographic influences across coarser scales and over longer time periods.

Acknowledgments

This research was funded by a Natural Sciences and Engineering Research Council of Canada (NSERC) Discovery Grant to IFC and a Canadian Foundation for Climate and Atmospheric Sciences (CFCAS) Grant to IFC, FDB, and RAB. We acknowledge the efforts of university students and government technicians from Natural Resources Canada and Environment Canada for assisting in the collection and analyses of the soils.

References

Beall, F.D., Semkin, R.G., Jeffries, D.S., 2001. Trends in the output of first-order basins at Turkey Lakes Watershed, 1982–96. Ecosystems 4, 514–526.
Becker, A., Braun, P., 1999. Disaggregation, aggregation and spatial scaling in hydrological modeling. J. Hydrol. 217, 239–252.
Bedard-Haughn, A.K., Pennock, D.J., 2002. Terrain controls on depressional soil distribution in a hummocky morainal landscape. Geoderma 110, 169–190.
Benayas, J.M.R., Sánchez-Colomer, M.G., Escudero, A., 2004. Landscape- and field-scale control of spatial variation of soil properties in Mediterranean montane meadows. Biogeochemistry 69, 207–225.
Beven, K.J., Kirkby, M.J., 1979. A physically based, variable contributing area model of basin hydrology. Hydrol. Sci. Bull. 24, 43–69.
Bourbonnière, R.A., Creed, I.F., 2006. Biodegradability of dissolved organic matter extracted from a chronosequence of forest-floor materials. J. Plant Nutr. Soil Sc. 169, 101–107.
Burrough, P.A., MacMillan, R.A., van Deursen, W., 1992. Fuzzy classification methods for determining land suitability from soil profile observations and topography. J. Soil Sci. 43, 193–210.
Chen, J.M., Govind, A., Sonnentag, O., Zhang, Y.Q., Barr, A., Amiro, B., 2006. Leaf area index measurements at Fluxnet-Canada forest sites. Agr. For. Meteorol. 140, 257–268.
Churkina, G., Running, S.W., 1998. Contrasting climatic controls on the estimated productivity of global terrestrial biomes. Ecosystems 1, 206–215.
Clark, R.B., Creed, I.F., Sass, G.Z., 2009. Mapping hydrologically sensitive areas on the boreal plain: a multitemporal analysis of ERS synthetic aperture radar data. Int. J. Remote Sens. 30, 2619–2635.
Conacher, A.J., Dalrymple, J.B., 1977. The nine unit land surface model: an approach to pedogeomorphic research. Geoderma 18, 1–153.
Corporation, Microsoft, 2003. Office Excel 2003 for Windows XP. Redmond, Washington, USA.
Creed, I.F., Trick, C.G., Band, L.E., Morrison, I.K., 2002. Characterizing the spatial pattern of soil carbon and nitrogen pools in the Turkey Lakes Watershed: a comparison of regression techniques. Water Air Soil Poll. Focus 2, 81–102.
Creed, I.F., Sanford, S.E., Beall, F.D., Molot, L.A., Dillon, P.J., 2003. Cryptic wetlands: integrating hidden wetlands in regression models of the export of dissolved organic carbon from forested landscapes. Hydrol. Process. 17, 3629–3648.
Creed, I.F., Beall, F.D., Clair, T.A., Dillon, P.J., Husslein, R.H., 2008. Predicting export of dissolved organic carbon from forested catchments in glaciated landscapes with shallow soils. Glob. Biogeochem. Cy. 22, GB4024.
Finzi, A.C., Van Breemen, N., Canham, C.D., 1998. Canopy tree soil interactions within temperate forests: species effects on soil carbon and nitrogen. Ecol. Appl. 8, 440–446.
Gaudinski, J.B., Trumbore, S.E., Davidson, E.A., Zheng, S., 2000. Soil carbon cycling in temperate forest: radiocarbon-based estimates of residence times, sequestration rates and partitioning of fluxes. Biogeochemistry 51, 33–69.
Gessler, P.E., Chadwick, O.A., Chamran, F., Althouse, L., Holmes, K., 2000. Modeling soil-landscape and ecosystem properties using terrain attributes. Soil Sci. Soc. Am. J. 64, 2046–2056.
Hall, G.F., Olson, C.G., 1991. Predicting variability of soils from landscape models. In: Manusbach, M.J., Wilding, L.P. (Eds.), Spatial Variabilities of Soils and Landforms. Soil Sci. Soc. Am. J. Special Publication, No. 28, Madison, WI, pp. 9–24.
Jeffries, D.S., 2002. Foreword. The Turkey Lakes Watershed study after two decades. Water Air Soil Poll. Focus 2, 1–3.
Jeffries, D.S., Foster, N.W., 2001. The Turkey Lakes Watershed study: milestones and prospects. Ecosystems 4, 501–502.
Jeffries, D.S., Kelso, J., Morrison, I.K., 1988. Physical, chemical and biological characteristics of the Turkey Lakes Watershed, central Ontario. Can. J. Fish. Aquat. Sci 45, 3–13.
Jeglum, J.R., Rothwell, R.L., Berry, G.J., Smith, G.K.M., 1992. A Peat Sampler for Rapid Survey, Canadian Forest Service – Sault Ste. Marie, Ontario. Frontline Technical Note.
Jenny, H., 1941. Factors of soil formation: a system of quantitative pedology. N.Y., McGraw-Hill Publishers, New York.
Johnson, D.W., Lindberg, S.E., 1992. Atmospheric deposition and nutrient cycling: a synthesis of the integrated forest study. Springer, New York.

Laiho, R., 2006. Decomposition in peatlands: reconciling seemingly contrasting results on the impacts of lowered water levels. Soil Biol. Biochem. 38, 2011–2024.
Lauren, A., Mannerkoski, H., 2001. Hydraulic properties of mor layers in Finland. Scand. J. For. Res. 16, 429–441.
Lee, D., Yoo, G., Oh, S., Shim, J.H., Kang, S., 1999. Significance of aspect and understory to leaf litter redistribution in a temperate hardwood forest. Korean J. Biol. Sci. 3, 143–147.
Li, P.H., Wang, Q., Endo, T., Zhao, X., Kakubari, Y., 2010. Soil organic carbon stock is closely related to aboveground vegetation properties in cold-temperate mountainous forests. Geoderma 154, 407–415.
Li-Cor, 2004. LAI-2000 Plant Canopy Analyzer Operating Manual. Li-cor Biosciences, Lincoln, Nebraska USA.
Lim, K., Treitz, P., Baldwin, K., Morrison, I., Green, J., 2003a. LiDAR remote sensing of biophysical properties of tolerant northern hardwood forests. Can. J. Remote Sens. 29, 658–678.
Lim, K., Treitz, P., Wulder, M., St-Onge, B., Flood, M., 2003b. LiDAR remote sensing of forest structure. Prog. Phys. Geog. 27, 88–106.
Lindsay, J.B., 2005. Terrain Analysis System version 2.0.9.
Lindsay, J.B., Creed, I.F., 2006. Distinguishing actual and artifact depressions in digital elevation data. Comput. Geosci. 32, 1192–1204.
MacMillan, R.A., Pettapiece, W.W., Nolan, S.C., Goddard, T.W., 2000. A generic procedure for automatically segmenting landforms into landform elements using DEMs, heuristic rules and fuzzy logic. Fuzzy Set. Syst. 113, 81–109.
Martin, W.K.E., Timmer, V.R., 2006. Capturing spatial variability of soil and litter properties in a forest stand by landform segmentation procedures. Geoderma 132, 169–181.
McClain, M.E., Boyer, E.W., Dent, C.L., Gergel, S.E., Grimm, N.B., Groffman, P.M., Hart, S.C., Harvey, J.W., Johnston, C.A., Mayorga, E., McDowell, W.H., Pinay, G., 2003. Biogeochemical hot spots and hot moments at the interface of terrestrial and aquatic ecosystems. Ecosystems 6, 301–312.
McKenzie, N.J., Ryan, P.J., 1999. Spatial prediction of soil properties using environmental correlation. Geoderma 89, 67–94.
Moore, I.D., Gessler, P.E., Nielsen, G.A., Peterson, G.A., 1993. Soil attribute prediction using terrain analysis. Soil Sci. Soc. Am. J. 57, 443–452.
Morrison, I.K., 1990. Organic matter and mineral distribution in an old-growth *Acer saccharum* forest near the northern limit of its range. Can. J. For. Res. 20, 1332–1342.
Morrison, I.K., Foster, N.W., 2001. Fifteen-year change in forest floor organic and element content and cycling at the Turkey Lake Watershed. Ecosystems 4, 545–554.
O'Callaghan, J.F., Mark, D.M., 1984. The extraction of drainage networks from digital elevation data. Comput. Vis. Graph. 28, 323–344.
Orndorff, K.A., Lang, G.E., 1981. Leaf litter redistribution in a West Virginia hardwood forest. J. Ecol. 69, 235–255.
Park, S.J., van de Giesen, N., 2004. Soil-landscape delineation to define spatial sampling domains for hillslope hydrology. J. Hydrol. 295, 28–46.
Park, S.J., Vlek, P.L.G., 2002. Environmental correlation of three-dimensional soil spatial variability: a comparison of three adaptive techniques. Geoderma 109, 117–140.
Park, S.J., McSweeney, K., Lowery, B., 2001. Identification of the spatial distribution of soils using a process-based terrain characterization. Geoderma 103, 249–272.
Pennock, D.J., Zebarth, B.J., De Jong, E., 1987. Landform classification and soil distribution in hummocky terrain, Saskatchewan, Canada. Geoderma 40, 297–315.
Planchon, O., Darboux, F., 2002. A fast, simple and versatile algorithm to fill the depressions of digital elevation models. Catena 46, 159–176.
Qi, F., Zhu, A.-X., Harrower, M., Burt, J.E., 2006. Fuzzy soil mapping based on prototype category theory. Geoderma 136, 774–787.
Rezaei, S.A., Gilkes, R.J., 2005. The effects of landscape attributes and plant community on soil chemical properties in rangelands. Geoderma 125, 167–176.
Rosenbloom, N.A., Harden, J.W., Neff, J.C., Schimel, D.S., 2006. Geomorphic control of landscape carbon accumulation. J. Geophys. Res. Biogeo. 111 (G1), G01004.
Schmidt, J., Hewitt, A., 2004. Fuzzy land element classification from DTMs based on geometry and terrain position. Geoderma 121, 243–256.
Soil Classification Working Group, 1998. The Canadian system of soil classification, 3rd Edition. Agriculture and Agri-Food Canada, Ottawa, Ontario.
Systat Software Inc, 2008. SigmaPlot, Version 11, Chicago, IL, USA.
Tarboton, D.G., 1997. A new method for the determination of flow directions and upslope areas in grid digital elevation models. Water Resour. Res. 33, 309–319.
Watson, R., Noble, I., Bolin, B., Ravindranath, N.H., Verardo, D., Andrasko, K., Apps, M., Brown, S., Farquhar, G., Goldberg, D., Hamburg, S., Houghton, R., Jarvis, P., Karjalainen, T., Kheshgi, H., Krug, T., Kurz, W., Lashof, D., Lim, B., Makundi, W., Manning, M., Marland, G., Masera, O., Murdiyarso, D., Murray, B., Persson, R., Sampson, N., Sathaye, J., Scholes, R., Schlamadinger, B., Sombroek, W., Prisley, S., Stone, J., Sukumar, R., Valentini, R., 2000. Summary for policymakers: land-use, land-use change, and forestry. IPCC Special Report. 92-9169-114-3.
Webster, K.L., Creed, I.F., Bourbonnière, R.A., Beall, F.D., 2008a. Controls on the heterogeneity of soil respiration in a tolerant hardwood forest. J. Geophys. Res. Biogeo. 113, G03018.
Webster, K.L., Creed, I.F., Beall, F.D., Bourbonnière, R.A., 2008b. Sensitivity of catchment-aggregated estimates of soil carbon dioxide efflux to topography under different climatic conditions. J. Geophys. Res. Biogeo. 113, G03040.
White, M.A., Asner, G.P., Nemani, R.R., Privette, J.L., Running, S.W., 2000. Measuring fractional cover and leaf area index in arid ecosystems: digital camera, radiation transmittance, and laser altimetry methods. Remote Sens. Environ. 74, 45–57.
Wickware ,, G.M., Cowell, D.W., 1985. Forest ecosystem classification of the Turkey Lakes Watershed. Ecological Classification Series No. 18. Lands Directorate, Environment Canada, Ottawa.
Wilson, J.P., Gallant, J.C., 2000. Secondary topographic attributes. In: Wilson, J.P., Gallant, J.C. (Eds.), Terrain Analysis: Principles and Applications. John Wiley and Sons, New York, pp. 87–131.
Xiong, S.J., Nilsson, C., 1997. Dynamics of leaf litter accumulation and its effects on riparian vegetation: a review. Bot. Rev. 63, 240–264.
Young, A., 1972. The soil catena: a systematic approach. In: International geography. In: Adams, W.P., Helleiner, F.M. (Eds.), International Geography Congress, Vol. 1. University of Toronto Press, Toronto, Canada, pp. 287–289.
Ziadat, F.M., 2005. Analyzing digital terrain attributes to predict soil attributes for a relatively large area. Soil Sci. Soc. Am. J. 69, 1590–1599.
Zhu, A.X., Band, L.E., 1994. A knowledge-based approach to data integration for soil mapping. Can. J. Remote Sens. 20, 408–418.
Zhu, A.X., Moore, A.C., Smith, M.P., Liu, J., Burt, J.E., Qi, F., Simonson, D., Hempel, J., Lubich, K., 2004. Advance in information technology for soil surveys: the SoLIM effort. In: Eswaran, H., Vijarnsorn, P., Vearasilp, T., Padmanabhan, E. (Eds.), Innovative Techniques in Soil Survey: Developing the Foundation for a New Generation of Soil Resource Inventories and Their Utilization. Land Development Department, Bangkok, Thailand, pp. 25–42.
Zushi, K., 2006. Spatial distribution of soil carbon and nitrogen storage and forest productivity in a watershed planted to Japanese cedar (*Cryptomeria japonica* D. Don). J. For. Res. Jpn. 11, 351–358.